Drug and Chemical Toxicology

ISSN: (Print) (Online) Journal homepage: https://www.tandfonline.com/loi/idct20

Pterocarpus mildbraedii leaf extract ebbs propanil-induced oxidative and apoptotic damage in the liver of rats

Chiagoziem A. Otuechere & Ebenezer O. Farombi

To cite this article: Chiagoziem A. Otuechere & Ebenezer O. Farombi (2020): *Pterocarpus mildbraedii* leaf extract ebbs propanil-induced oxidative and apoptotic damage in the liver of rats, Drug and Chemical Toxicology, DOI: 10.1080/01480545.2020.1842884

To link to this article: https://doi.org/10.1080/01480545.2020.1842884

DRUG AND CHEMICAL TOXICOLOGY
https://doi.org/10.1080/01480545.2020.1842884

Taylor & Francis
Taylor & Francis Group

ARTICLE

Pterocarpus mildbraedii leaf extract ebbs propanil-induced oxidative and apoptotic damage in the liver of rats

Chiagoziem A. Otuechere[a,b] and Ebenezer O. Farombi[b]

[a]Department of Biochemistry, Faculty of Basic Medical Sciences, Redeemer's University, Ede, Nigeria; [b]Department of Biochemistry, Faculty of Basic Medical Sciences, University of Ibadan, Ibadan, Nigeria

ABSTRACT

Phytochemicals derived from plant sources are well recognized as sources of pharmacologically potent drugs in the treatment of several oxidative stress-related ailments. Dichloromethane/methanol (1:1) leaf extract of *Pterocarpus mildbraedii* was evaluated for its possible protection against oxidative stress and apoptosis in the liver of male Wistar rats exposed to propanil (PRP). In the experimental design, olive oil served as the vehicle, and rats were grouped into control (2 mL/kg olive oil), PRP (200 mg/kg/day), *Pterocarpus mildbraedii* extract (200 mg/kg/day), and *Pterocarpus mildbraedii* extract (200 mg/kg/day)+PRP (200 mg/kg/day), and treated daily, p.o., for seven days. Oxidative stress parameters, B-cell lymphoma 2 (Bcl-2), Bcl 2-associated X protein (Bax), p53, caspases (9/3), and terminal transferase dUTP nick end labeling (TUNEL) assays were observed in all groups. Propanil significantly elevated superoxide dismutase and lipid peroxidation levels, while concomitantly depleting GSH and p53 levels. Further, PRP enhanced the expressions of caspase-9, caspase-3, Bax, and TUNEL-positive cells in the liver of rats. However, these observed alterations were reversed following treatment with *Pterocarpus mildbraedii* extract. Our studies suggest that *Pterocarpus mildbraedii* extract protected against PRP toxicity by reducing oxidative stress and attenuating critical endpoints in the intrinsic apoptotic pathway.

ARTICLE HISTORY
Received 9 July 2020
Revised 13 October 2020
Accepted 18 October 2020

KEYWORDS
Dichloromethane/methanol; *Pterocarpus mildbraedii*; propanil; oxidative stress; Bax; caspases; rats

Introduction

Recently, the adverse effects of environmental chemicals on the liver have become increasingly prominent, and the level of exposure to these chemicals varies from minute quantities to very high doses. Hepatic injury to animals could arise from direct exposure to toxicants, altered immune mechanisms, or biotransformation processes (Dalhoff 2017). Propanil (PRP), an acylanilide herbicide widely used in grain fields, is the product of a hydrogen-catalyzed-reaction between 1, 2-dichlorobenzene, and acetyl chloride hydrogen (Moore and Farris 1997, Wyatt and Paul 2008). Statistics revealed that applied pesticides spread beyond their intended targets, and in the process might produce deleterious effects on non-target organisms, including humans (Carvalho 2017). Pesticide-induced toxicities could arise through various mechanisms, including redox imbalance and apoptosis (Franco *et al.* 2009, Elsharkawy *et al.* 2013). Excessive production of free radicals depletes the antioxidant molecules and further induces an imbalance between the antioxidant defense system and free radicals culminating into oxidative stress-mediated damage (Singh and Sharma 2019).

Apoptosis, also known as programmed cell death, has been implicated in various liver diseases. Apoptosis is particularly useful in removing damaged or infected cells that may impede physiological function. The intrinsic apoptotic pathway involves the release of cytochrome c from the mitochondria resulting in the formation of the apoptosome. Subsequently, caspases 9 and 3, representing the initiator and executioner caspases, respectively, are activated (Pfeffer and Singh 2018, Mccomb *et al.* 2019). Phytomedicine, presumably causing minimal side effects in patients, has emerged as an important source of antioxidants that could be exploited in the treatment of various diseases, including hepatotoxicity (Gupta and Sharma 2017). For example, an aqueous leaf extract of *Aloe vera* administered p.o. at a dose of 420 mg/kg, for 15 days, ameliorated cartap, and malathion-induced toxicities in the liver of rats (Gupta *et al.* 2020). On the other hand, *Pterocarpus mildbraedii* is used traditionally to treat headaches, pains, fever, and convulsions, and other respiratory disorders. The leaves from *Pterocarpus mildbraedii* have also been reported to possess anti-inflammatory, antibacterial properties, and protective effects against diabetes (Omale and Ugwu 2011, Otuechere and Farombi 2020). Partially purified fractions of *Pterocarpus mildbraedii* have been reported to possess some antioxidant activity, which suggests its usefulness in the treatment of diseases, especially the liver-borne diseases (Hamzah *et al.* 2018). The present work was, therefore, carried out in order to evaluate the impact of PRP, and also to monitor the ameliorating effect, if any, of the dichloromethane/methanol leaf extract of *Pterocarpus mildbraedii* in the liver of rats.

CONTACT Ebenezer O. Farombi olatunde_farombi@yahoo.com Department of Biochemistry, Faculty of Basic Medical Sciences, University of Ibadan, Ibadan, Nigeria

Materials and methods

Chemicals and reagents

Technical grade PRP (99.5% purity) under the trade name Vespanil® 36 EC (CAS no.: 909-98-8) was obtained from an agro shop in Lagos State, Nigeria. Bax, B-cell lymphoma 2 (Bcl-2), caspase-3, caspase-9, antibodies (Abcam, Cambridge, UK), TUNEL assay kit (Promega, Madison, WI), and p53 and phospho p53 ELISA kits (Cell Signaling Technology, Boston, MA) were also purchased. All other analytical grade chemicals were obtained from Sigma-Aldrich (St. Louis, MO).

Plant sourcing and extract preparation

Pterocarpus mildbraedii leaves were bought from a local market in Lagos State, Nigeria. They were taxonomically identified and documented with the voucher number LUT/5913 at the Herbarium of the Department of Botany, University of Lagos, Lagos, Nigeria. The pulverized plant material weighing 235.7 g was packed into a soxhlet extractor and extracted with two solvents dichloromethane and methanol (1:1). The fraction obtained was then concentrated *in vacuo* to yield a black syrupy extract weighing 99.1 g. Prior to animal treatments, the stock solution of PME (100 mg/mL) was prepared with olive oil, while the concentrate was analyzed using Fourier transform infrared (FTIR) spectroscopy.

Preliminary phytochemicals studies

Determination of total phenolic compounds. The total phenolic content of PME was determined according to the method described by Yen *et al.* (2001). Briefly, 0.1 g of the extract was dissolved in 5 mL of 0.3% HCl in methanol/water (60:40, v/v). The resulting solution (100 µL) was then added to 2 mL of 2% Na_2CO_3. After 2 min, 100 µL Folin–Ciocalteau reagent was added to the mixture and allowed to stand for 30 min. Absorbance was measured at 750 nm, and the total phenolic contents were calculated as Gallic acid equivalents.

Determination of total flavonoid content. The total flavonoid content of PME was determined by the aluminum chloride colorimetric method, as described by Chang *et al.* (2020). Briefly, extract (500 µL) was mixed with methanol (1.5 mL), aluminum chloride (100 µL), 1 M potassium acetate (100 µL), and distilled water (2.8 mL). The mixture was incubated at room temperature for 40 min, and the absorbance was measured at 415 nm. The total flavonoid content was expressed as Gallic acid equivalents mg/g dry weight.

Animal husbandry and experimental design. Albino rats were procured from the animal house of the Department of Veterinary Anatomy, University of Ibadan. Animals were maintained on standard chow and given unfettered access to drinking water *ad libitum* maintained under the 12 h light and 12 h dark photoperiod. Animals were treated benignantly according to the National Research Council guidelines (NRC 2011) as approved by the University of Ibadan Ethical Committee, with the study code as S.I. 68021. Twenty-four male rats used in the study were as grouped into four as follows: control (2 mL/kg olive oil), PRP (200 mg/kg/day, p.o.), PME (200 mg/kg/day, p.o.), and PME (200 mg/kg/day, p.o.)+PRP (200 mg/kg/day, p.o.). Experiments lasted for seven days, and the dose for PRP was selected based on a prior study in our laboratories (Otuechere *et al.* 2019). Further, the dose of 200 mg/kg PME was based on a previous study with ethanol and aqueous extracts of *Pterocarpus mildbraedii* (Adegbite 2015). However, an equimolar mixture of dichloromethane/methanol was used in this study in order to extract more lipophilic compounds from the plant leaves.

Assessment of oxidative stress parameters. The liver was excised, rinsed with chilled 1.15% KCl solution, and homogenized in 4 volumes of 0.1 M phosphate buffer (pH 7.4). Centrifugation of the resulting homogenates was performed at 4500×*g* for 20 min to obtain a supernatant, which was stored until further analysis. Total protein concentrations were determined based on the method of Gornall *et al.* (1949), while the superoxide dismutase (SOD) activity was determined in a mixture of the sample (0.02 mL), epinephrine (3 mL), and sodium carbonate buffer (2.5 mL) at the wavelength of 480 nm (Misra and Fridovich 1972). Catalase (CAT) was assayed using hydrogen peroxide as a substrate in the presence of 0.01 M phosphate buffer (Sinha 1972). Briefly, 0.1 mL of the sample, 0.5 mL H_2O_2, and phosphate buffer were incubated for 15 min, followed by the addition of 5% dichromate solution. Absorbance was determined at 570 nm, and CAT activity was calculated in terms of the amount of H_2O_2 consumed. Reduced glutathione (GSH) levels were determined using 5, 5′-dithiobis (2-nitrobenzoic) acid (DTNB) as substrate as previously described (Beutler *et al.* 1963). Briefly, a reaction mixture containing the sample (0.2 mL), sulfosalicylic acid (3.3 mL), and distilled water (1.5 mL) was filtered for 5 min followed by the addition of 0.5 mL DTNB in phosphate buffer. Absorbance was then recorded at 412 nm after 15 min. Lipid peroxidation, quantified as malondialdehyde (MDA), was determined according to the protocol of Varshney and Kale (1990). The reaction mixture containing thiobarbituric acid and trichloroacetic acid was incubated at 80 °C, and absorbance was measured obtained at 532 nm.

Analysis of p53 and phospho p53. Sandwich ELISA procedure was used to quantify protein levels of p53 and phospho-p53 (ser15) according to the manufacturer's manual. Briefly, diluted liver lysates were introduced into a 96-well plate, already pre-coated with primary antibodies, and incubated for 2 h at 37 °C. After further 60 min incubation with corresponding detection antibodies and horseradish peroxidase (HRP)-linked secondary antibodies, 3, 3′, 5, 5′-tetramethylbenzidine was added. The absorbance was taken at 450 nm.

Histological and gross examinations. Livers from rats of all the groups were fixed in 10% formaldehyde, dehydrated in graded alcohol, and embedded in paraffin. Fine sections were obtained, mounted on glass slides, and counter-stained with hematoxylin–eosin (H&E) for light microscopic analyses.

The slides were examined by a histopathologist blinded to the treatment groups.

Analysis of caspase-9, caspase-3, Bax, and Bcl-2 by immunohistochemistry. Three representative liver sections per group were fixed in formal saline. Subsequently, they were incubated overnight in a humidified chamber, using the primary rabbit monoclonal antibodies: caspase-9, caspase-3, Bcl-2, and Bax. Further incubations with biotin-labeled secondary antibody and HRP-conjugated streptavidin followed. 3, 3′-Diaminobenzidine tetrahydrochloride was used for staining.

Terminal de-oxy nucleotidyl transferase-mediated dUTP nick end-labeled (TUNEL) assay. The TUNEL assay kit was used to detect apoptotic cells according to the manufacturer's instructions. The assay involved the removal of paraffin, several rehydration steps, fixing in buffered paraformaldehyde solution, and treatment with proteinase K. After incubation with the equilibration buffer, the sections were allowed to react with the rTDT reaction mixture. Endogenous peroxidase activity was blocked by using H_2O_2, followed by further incubation with a streptavidin-HRP solution for 30 min at room temperature. 3, 3′-Diaminobenzidine tetrahydrochloride was used for staining. Darkly stained nuclei, visualized by microscopy, were counted as positive.

Statistical analysis

Data are presented as mean ± SEM. Comparisons between the groups were determined by one-way analysis of variance and Tukey's *post hoc* test (GraphPad Prism, version 8, La Jolla, CA). $p < 0.05$ was considered as significant.

Results

Preliminary phytochemical studies

The phytochemical studies revealed a yield of 42.04% of the dichloromethane/methanol leaf extract of *Pterocarpus mildbraedii*. The level/g of dry extract of total phenols was 0.22 mg GAE, while that of the total flavonoids was 0.08 mg GAE (Table 1).

Effect of PME on propanil-induced oxidative stress markers

The effect of PME on selected oxidative stress markers in the liver of rats exposed to PRP is shown in Figure 1. The SOD activity significantly increased in rats exposed to PRP compared with the control group. PME prevented PRP-induced increase in SOD activity. Contrariwise, there was no significant change in the CAT activity of the rats exposed to PRP. PRP treatment also significantly depressed GSH levels and elevated MDA levels when compared with the control group. However, treatment with PME + PRP reversed the alterations in GSH and MDA levels back to normal.

Table 1. Total phenolic and flavonoid contents of *Pterocarpus mildbraedii* (PME) extract.

Extract	Total phenolic content (mg/g GAE)	Total flavonoid content (mg/g GAE)
PME	0.22 ± 0.01	0.08 ± 0.003

GAE: gallic acid equivalent.
Values are expressed as means of three replicates ± SEM.

Effect of PME and PRP treatment on hepatic p53 and phospho-p53 levels

The effects of PME and PRP on hepatic p53 and phospho-p53 levels are depicted in Figure 2. There were significant ($p < 0.05$) and non-significant decreases in the total p53 and phospho-p53 levels, respectively, in PRP-treated rats compared with the controls. However, co-treatment with PME + PRP restored phospho-p53 levels to near normal values when compared with the PRP group.

Effect of PME and PRP treatment on hepatic histopathology

Liver sections revealed no visible lesions in the control group, but there were severe periportal infiltrations and fibroplasia in the group treated with PRP. Co-treatment of PME + PRP reduced the severity of these histopathological changes (Figure 3(A–D)). The gross morphological appearance of the liver in the PRP treated group showed the presence of white pustular nodules (arrowhead), which was ameliorated by the treatment with PME (Figure 3(E–H)).

Effect of PME and PRP treatment on hepatic caspase-9, caspase-3, Bax, and Bcl-2 levels

Immunohistochemical evaluation showing the effects of the treatment of PME on caspase-9 and caspase-3 expressions in the liver of PRP-treated rats is shown in Figure 4(A–H). PRP elicited more intense expressions of caspases-9 and -3 expressions than the control groups. Co-treatment with PME + PRP decreased the expressions of these proteins. The expressions of Bax and Bcl-2 in rats exposed to PRP were also stronger compared to the control groups. However, there were minimal expressions of these apoptotic proteins in the PME + PRP treatment groups (Figure 5(A–H)).

Effect of PME and PRP treatment on TUNEL-positive nuclei

Assessment of TUNEL-positive nuclei for all the treatment groups is represented in Figure 6(A–D). TUNEL-positive nuclei were not conspicuous in the control group. However, positive nuclei were more evident in the PRP compared to the control group. Co-treatment with PME + PRP reduced the number of positive nuclei compared to the PRP group.

Fourier transform analysis of Pterocarpus mildbraedii extract

Figure 7 shows the FTIR spectra of PME indicated the presence of O–H stretching vibration of alcohol at 3450 cm^{-1}, aliphatic C–H stretching vibrations at 2918 and 2848 cm^{-1}

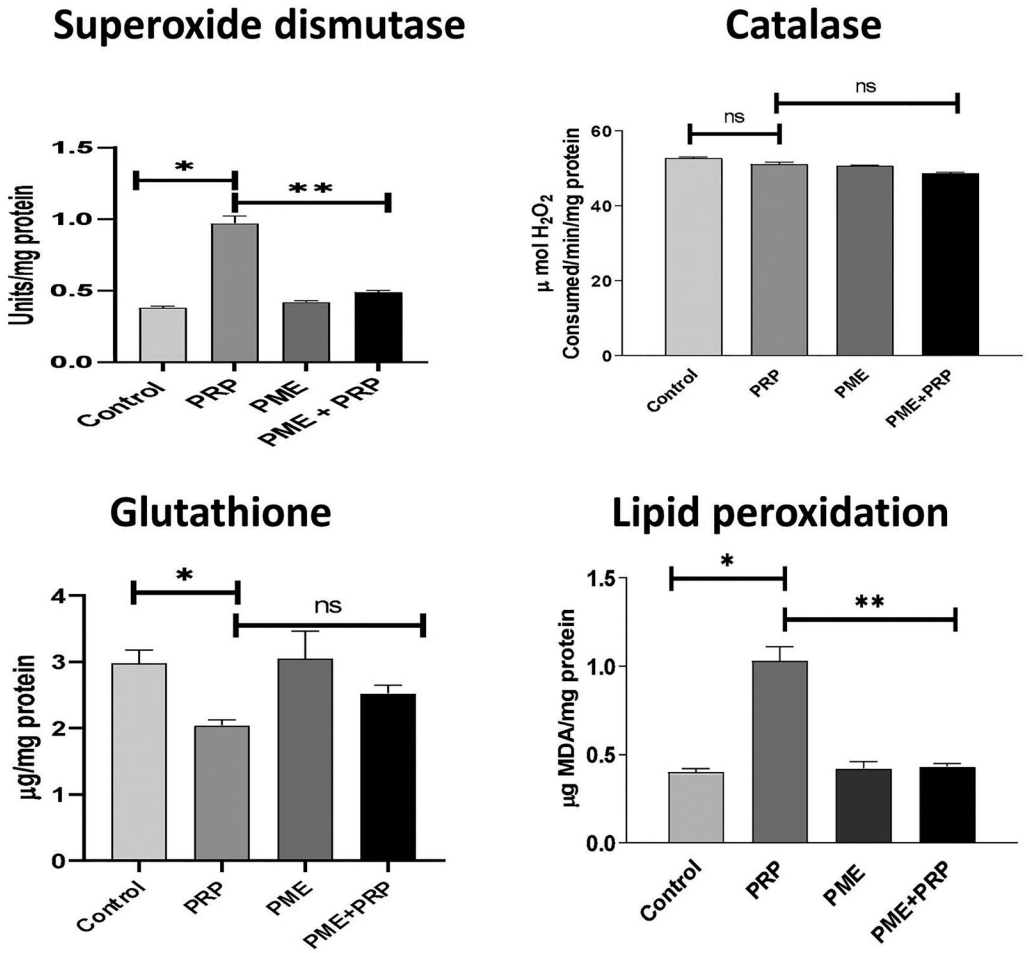

Figure 1. Effect of *Pterocarpus mildbraedii* (PME) extract on SOD, CAT, GSH, and LPO levels in the liver of PRP-exposed rats. Each bar represents mean ± SEM of five animals. *Values differ significantly from control ($p < 0.001$). **Values differ significantly from PRP ($p < 0.05$). PME: 200 mg/kg; propanil (PRP): 200 mg/kg. SOD: superoxide dismutase; CAT: catalase: GSH: glutathione; LPO: lipid peroxidation.

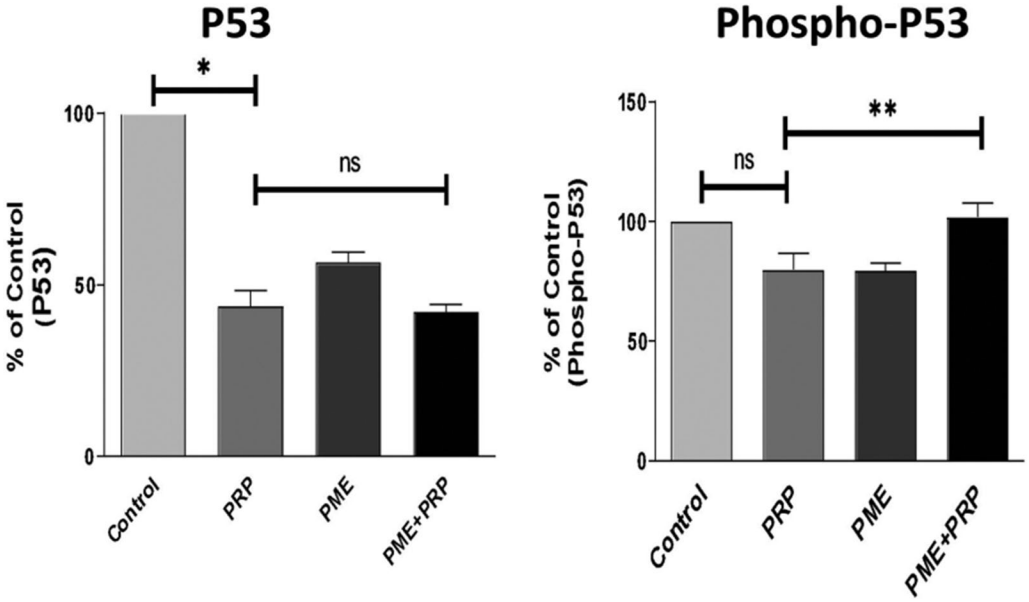

Figure 2. Effect of *Pterocarpus mildbraedii* (PME) extract on levels of p53 and phospho-p53 in PRP exposed rats. Results are expressed as a percentage of relative levels of phosphoproteins and are normalized to the control (100%). Values are mean ± SEM of technical duplicates. *Values differ significantly from control ($p < 0.001$). **Values differ significantly from PRP ($p < 0.05$).

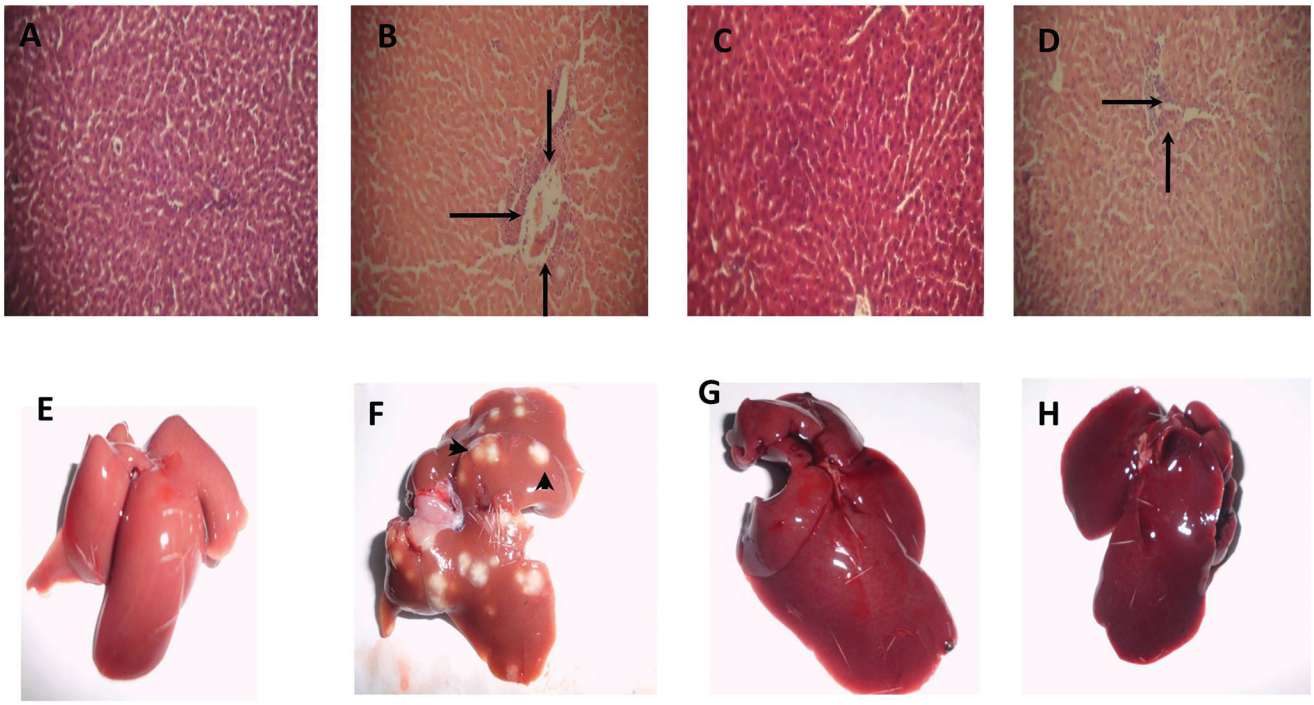

Figure 3. Representative photomicrographs of the liver. (A) Control showing normal architecture; (B) PRP group showing severe periportal cellular infiltration (arrow); (C) PME group with no visible lesion; (D) PME + PRP group showing moderate periportal cellular infiltration. Representative gross morphology of the liver. (E) Control with normal-looking morphology; (F) PRP group showing gross alterations and appearance of white nodules on the surface (arrowhead) of the liver; (G) PME group was showing a normal-looking appearance; (H) PME + PRP group with normal architecture, but vascularized appearance. Original magnification: ×400. PME: *Pterocarpus mildbraedii* extract; PRP: propanil.

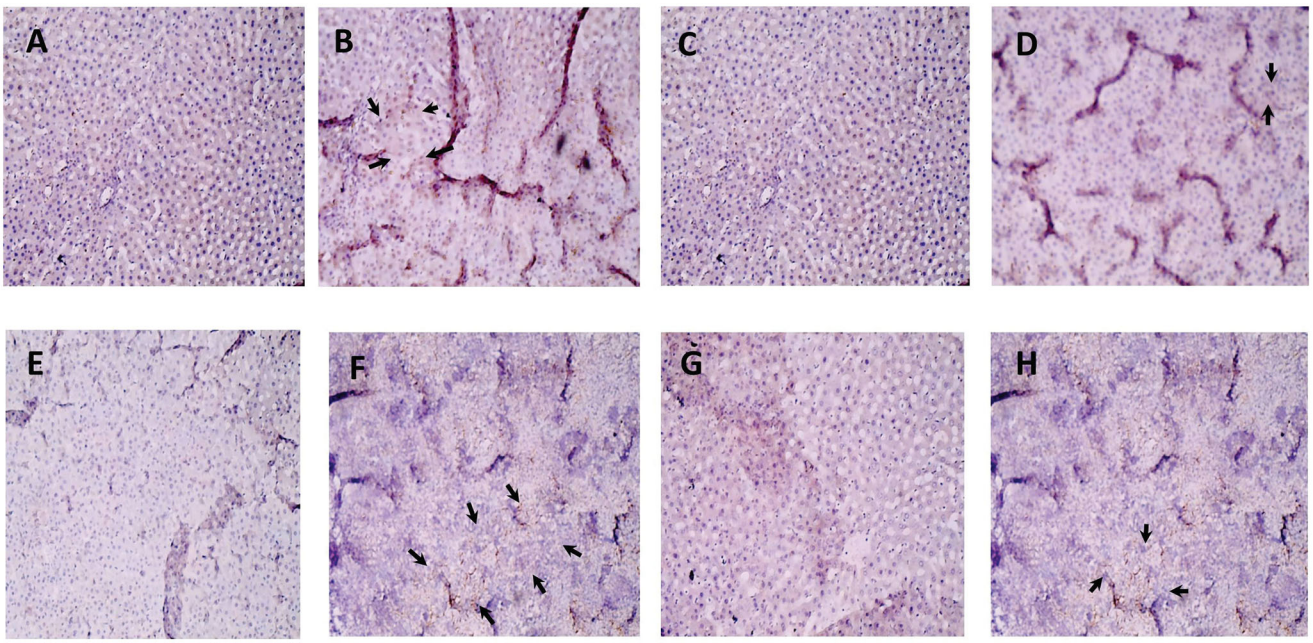

Figure 4. Immunohistochemistry of caspase 9 (A–D) and caspase 3 (E–H). (A) Control, (B) PRP, (C) PME, and (D) PME + PRP. Arrows in panels identify immunopositive cells. Original magnification: ×400.

corresponding to hydrogen bonds found predominantly in phenolic compounds. The band at 1634 cm^{-1} represents a weak –C=C– stretch of alkenes.

Discussion

Free radical-mediated oxidative stress has been suggested to be responsible for the toxicity of pesticides, and the peroxidation of lipid membranes is an indication of an alteration in the antioxidant: oxidant balance (Velki *et al.* 2019). Propanil-induced toxicity was associated with an elevation in SOD activity and a non-significant change in CAT activity in the liver. In a similar study, Dwivedi and Flora (2015) reported that a sub-chronic exposure of rats to arsenic and dichlorvos increased lipid peroxidation and SOD levels, while the CAT activity remained unchanged. In this study, the MDA level, an

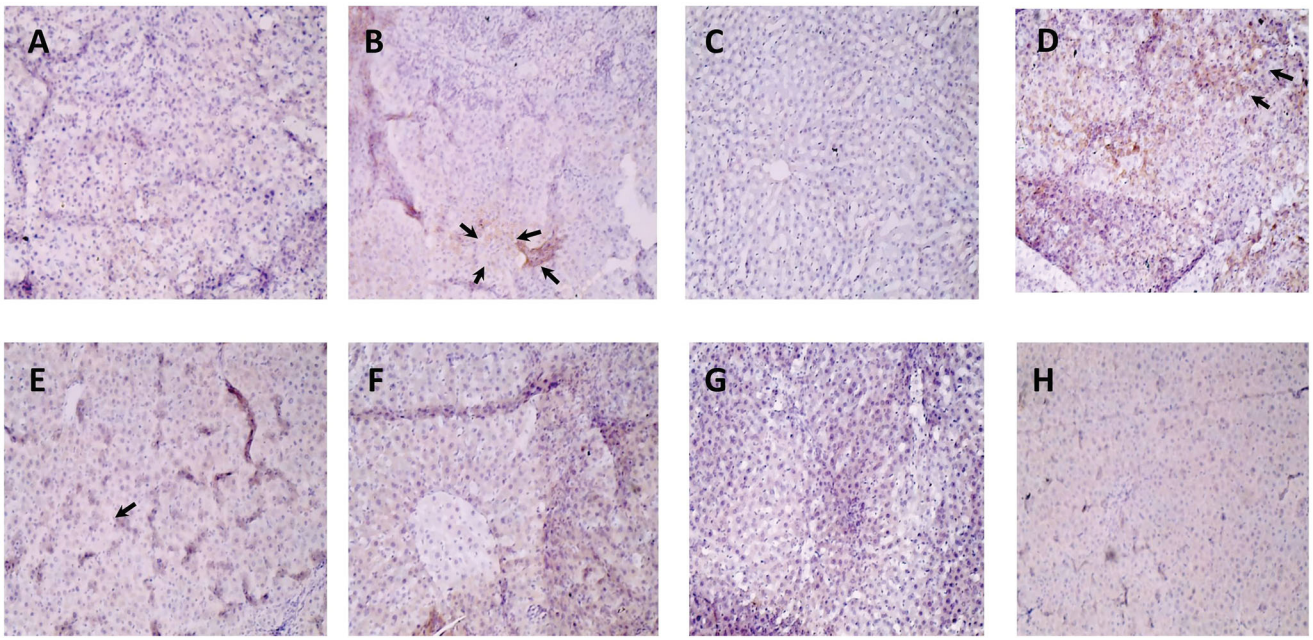

Figure 5. Immunohistochemistry of Bax (A–D) and Bcl-2 (E–H). (A) Control, (B) PRP, (C) PME, and (D) PME + PRP. Arrows in panels identify immunopositive cells. Original magnification: ×400.

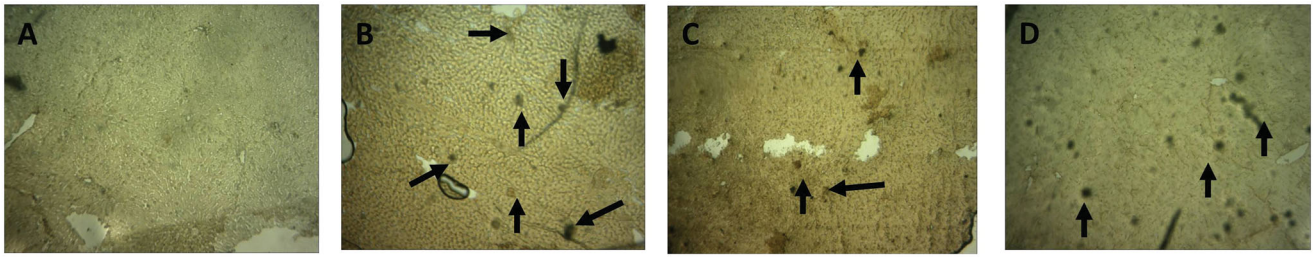

Figure 6. Liver histopathology guide showing the effect of *Pterocarpus mildbraedii* extract on PRP-induced apoptosis in rats. Arrows identify TUNEL-positive nuclei. Increased number of TUNEL-positive nuclei are seen in liver sections of PRP-treated rats. Original magnification ×400.

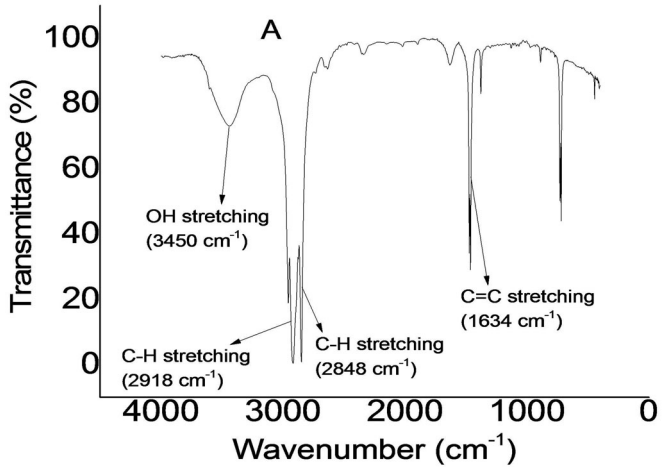

Figure 7. Fourier transform infrared (FTIR) spectroscopy of dichloromethane: methanol extract of *Pterocarpus mildbraedii*.

index of lipid peroxidation, was also increased in the PRP group. The decreased GSH levels observed after PRP intoxication is further evidence of an increase in free radical intermediates culminating in oxidative stress. Co-treatment of rats with PME + PRP led to a significant reduction in lipid peroxidation, which aligns with another study on the beneficial effects of *Crataegus oxyacantha* extract against deltamethrin and chlorpyrifos-induced increase in lipid peroxidation levels in rats (Saoudi *et al.* 2019). After seven days of the study, CAT activity was not significantly altered across all treatment groups, which may suggest an adaptive response to the increased dismutation of superoxide radicals by SOD.

Apart from oxidative stress, DNA damage and apoptosis have been implicated in the etiology of liver diseases (Jaeschke *et al.* 2018, Akazawa *et al.* 2019, Zhang *et al.* 2020). The apoptotic process could be initiated when the repair of DNA damage is slow or partial. Central to the initiation of apoptosis is p53, the so-called 'guardian of the genome' (Toufektchan and Toledo 2018). Experimental evidence exists suggesting that p53 could induce apoptosis by transcriptional up-regulation of pro-apoptotic genes such as *NOXA*, *PUMA*, and *BIM* (Ho *et al.* 2019). On the other hand, an alternative mechanism involving the translocation of p53 to the mitochondria where it associates with members of the BCL-2 family to induce membrane permeabilization and cytochrome c release, and subsequent downstream activation of the caspases has also been reported (Castrogiovanni *et al.* 2018, Udefa *et al.* 2020). In the present study, there were a higher proportion of TUNEL-positive nuclei cells in the PRP group, but these were diminished in the PME + PRP group. Our result is in

tandem with the anti-apoptotic effects of compounds of onion and garlic in a trichloromethane model of apoptosis in rats (Somade *et al.* 2018). Further, flavonoid and polyphenol containing medicinal plants via their free radical scavenging activities, have been reported to inhibit DNA damage (Singh and Sharma 2018).

PRP significantly down-regulated p53 expression but did not affect phospho-p53 levels, possibly suggesting that apoptosis proceeded via a mechanism independent of p-53 transcription (Ho *et al.* 2019). Furthermore, we investigated the effect of PME on PRP-induced alterations in apoptotic markers caspases 9 and 3, Bax, and Bcl-2. Pesticide-induced oxidative stress and its relationship with apoptosis mediated by intracellular caspases have been reported (Ojha and Gupta 2017, Owumi and Dim 2019). In the present study, we detected increased caspase-9 and caspase-3 activities in the liver of PRP-treated rats. The significant elevation of caspases-9 and -3 was abrogated close to normal in the group of rats co-treated with PME and PRP, indicating the possible anti-apoptotic effect of PME in the liver. This result is in line with a similar study in which a hydro-ethanolic extract of *Cyperus esculentus*, at the doses of 500 and 1000 mg/kg, down-regulated caspase-3 levels in the testes of rats fed with lead acetate (Udefa *et al.* 2020). The control and regulation of apoptotic mitochondrial events occur through members of the Bcl-2 family of proteins (Warren *et al.* 2019). In the present study, staining for Bax in liver tissues was significantly increased in rats given PRP. Our findings are similar to several reports from other groups concerning the mechanisms of apoptosis. For example, Ayan *et al*. (2013) demonstrated that Bax activities increased in livers of rats exposed to the organic solvent, toluene. Abarikwu and Farombi (2015) suggested that elevated expression of Bax contributed to apoptosis in SH-SY55 cells exposed to Atrazine. Since Bax is a protein involved in the mitochondrial pathway, it could be said that PRP leads to mitochondrial damage and thus activates the intrinsic pathway. As expected, Bcl-2 levels were down-regulated by PRP in the present study. Therefore, this alteration in the expression of Bax and Bcl-2 leads to a high Bax/Bcl-2 ratio, an important determinant of the cell's vulnerability to apoptosis. We also observed that PME mediated significant restoration in the PRP-induced alterations in the expression of Bax and Bcl-2 in the liver cells. These findings are in agreement with another report that showed that a dichloromethane fraction of *Corchorus olitorius* leaf increased Bcl-2 and decreased Bax expressions in an isoproterenol model of cardiotoxicity in rats (Alabi *et al.* 2020). Histopathological examination of liver sections from control groups showed normal parenchyma architecture, while the histoarchitecture in the liver of rats treated with PRP presented with severe periportal infiltrations and fibroplasia. Furthermore, exposure to PRP altered the gross histological appearance of the liver with the presence of white pustular nodules. Administration of PME ameliorated these PRP-induced morphological changes in the liver.

The bioactivity of the extract observed in this study could be as a result of the presence of phenols and flavonoids coupled with the presence of aliphatic compounds as identified by FTIR. This finding resonates with another study showing the hepatoprotective effect of partially purified sub-fractions of *Pterocarpus mildbraedii* extract (Hamzah *et al.* 2018).

Conclusions

In conclusion, this present study demonstrated that PME attenuated PRP-induced hepatic injury by its antioxidant and anti-apoptotic activities. The histological observations also affirm that PME protected the oxidative damage of the liver cells on account of its antioxidant potential.

Disclosure statement

The authors declare that there are no conflicts of interest. The present study was not conducted under contract with an agency of the Federal Government of Nigeria.

References

Abarikwu, S.O. and Farombi, E.O., 2015. Atrazine induces apoptosis of SH-SY5Y human neuroblastoma cells via the regulation of Bax/Bcl-2 ratio and caspase-3-dependent pathway. *Pesticide Biochemistry and Physiology*, 118, 90–98.

Adegbite, A.V., Ezekwesili, C.N., and Okani, O.C., 2015. Effects of ethanol and aqueous leaf extracts of *Pterocarpus mildbraedii* on the liver function and CD4 cells of the immune system in albino rats. *The Bioscientist*, 3, 79–87.

Akazawa, Y., *et al.*, 2019. Detection of DNA damage response in nonalcoholic fatty liver disease via p53-binding protein 1 nuclear expression. *Modern Pathology*, 32 (7), 997–1007.

Alabi, B., *et al.*, 2020. Protective effects and chemical composition of Corchorus olitorius leaf fractions against isoproterenol-induced myocardial injury through p65NFkB-dependent anti-apoptotic pathway in rats. *Journal of Basic and Clinical Physiology and Pharmacology*, 31 (5). doi:10.1515/jbcpp-2019-0108

Ayan, M., *et al.*, 2013. The apoptotic effect of a high dose of toluene on liver tissue during the acute phase: an experimental study. *Toxicology and Industrial Health*, 29 (8), 728–736.

Beutler, E., Duron, O., and Kelly, B.M., 1963. Improved method for the determination of blood glutathione. *The Journal of Laboratory and Clinical Medicine*, 61, 882–888.

Carvalho, F.P., 2017. Pesticides, environment, and food safety. *Food and Energy Security*, 6 (2), 48–60.

Castrogiovanni, C., *et al.*, 2018. Serine 392 phosphorylation modulates p53 mitochondrial translocation and transcription-independent apoptosis. *Cell Death and Differentiation*, 25 (1), 190–203.

Chang, C.C., *et al.*, 2020. Estimation of total flavonoid content in Propolis by two complementary colorimetric methods. *Journal of Food and Drug Analysis*, 10 (3), 178–182.

Dalhoff, K., *et al.*, 2017. Toxicant-induced hepatic injury. *In*: J. Brent, eds. *Critical care toxicology*. Switzerland: Springer International Publishing AG, 386–404.

Dwivedi, N. and Flora, S.J., 2015. Sub-chronic exposure to arsenic and dichlorvos on erythrocyte antioxidant defense systems and lipid peroxidation in rats. *Journal of Environmental Biology*, 36 (2), 383–391.

Elsharkawy, E.E., Yahia, D., and El-Nisr, N.A., 2013. Sub-chronic exposure to chlorpyrifos induces hematological, metabolic disorders and oxidative stress in rat: attenuation by glutathione. *Environmental Toxicology and Pharmacology*, 35 (2), 218–227.

Franco, R., *et al.*, 2009. Environmental toxicity, oxidative stress and apoptosis: ménage à trois. *Mutation Research*, 674 (1–2), 3–22.

Gornall, A.G., Bardawill, C.J., and David, M.M., 1949. Determination of serum protein by means of the biuret reaction. *The Journal of Biological Chemistry*, 177 (2), 751–756.

Gupta, V.K., *et al.*, 2020. Anti-inflammatory and antioxidative potential of *Aloe vera* on the cartap and malathion mediated toxicity in Wistar

rats. *International Journal of Environmental Research and Public Health*, 17 (14), 5177.

Gupta, V.K. and Sharma, B., 2017. Role of phytochemicals in neurotrophins mediated regulation of Alzheimer's disease. *International Journal of Complementary and Alternative Medicine*, 7 (4), 1–7.

Hamzah, R.U., *et al.*, 2018. Effect of partially purified sub-fractions of *Pterocarpus mildbraedii* extract on carbon tetrachloride intoxicated rats. *Integrative Medicine Research*, 7 (2), 149–158.

Ho, T., Tan, B.X., and Lane, D., 2019. How the other half lives: what p53 does when it is not being a transcription factor. *International Journal of Molecular Sciences*, 21 (1), 13.

Jaeschke, H., *et al.*, 2018. The role of apoptosis in acetaminophen hepatotoxicity. *Food and Chemical Toxicology*, 118, 709–718.

Mccomb, S., *et al.*, 2019. Efficient apoptosis requires feedback amplification of upstream apoptotic signals by effector caspase-3 or -7. *Science Advances*, 5 (7), eaau9433.

Misra, H.P. and Fridovich, I., 1972. The univalent reduction of oxygen by reduced flavins and quinines. *Journal of Biological Chemistry*, 247 (1), 188–192.

Moore, M.T. and Farris, J.L., 1997. Acute and chronic toxicity of the herbicide Stam M-4 in field and laboratory exposures. *Archives of Environmental Contamination and Toxicology*, 33 (2), 199–202.

NRC. 2011. *National Research Council Guidance for the Description of Animal Research in Scientific Publications. Institute for Laboratory Animal Research*. Washington, DC: National Academies Press (US).

Ojha, A. and Gupta, Y.K., 2017. Study of commonly used organophosphate pesticides that induced oxidative stress and apoptosis in peripheral blood lymphocytes of rats. *Human & Experimental Toxicology*, 36 (11), 1158–1168.

Omale, J. and Ugwu, C.E., 2011. Comparative studies on the protein and mineral composition of some selected Nigerian vegetables African. *Journal of Food Science*, 5, 22–25.

Otuechere, C.A., et al., 2019. Impact of an acylanilide herbicide propanil on biochemical indices in kidney of diabetic rats. *Asian Journal of Biological Sciences*, 12 (2), 210–216.

Otuechere, C. A. and Farombi, E. O., 2020. Pterocarpus mildbraedii (Harms) extract resolves propanil-induced hepatic injury via repression of inflammatory stress responses in Wistar rats. *Journal of Food Biochemistry*, e13506.

Owumi, S.E. and Dim, U.J., 2019. Manganese suppresses oxidative stress, inflammation, and caspase-3 activation in rats exposed to chlorpyrifos. *Toxicology Reports*, 6, 202–209.

Pfeffer, C.M. and Singh, A.T., 2018. Apoptosis: a target for anticancer therapy. *International Journal of Molecular Sciences*, 19, 448.

Saoudi, M., *et al.*, 2019. Beneficial effects of *Crataegus oxyacantha* extract on neurobehavioral deficits and brain tissue damages induced by an insecticide mixture of deltamethrin and chlorpyrifos in adult Wistar rats. *Biomedicine & Pharmacotherapy = Biomedecine & Pharmacotherapie*, 114, 108795.

Singh, N. and Sharma, B., 2018. Biotoxins mediated DNA damage and role of phytochemicals in DNA protection. *Biochemistry and Molecular Biology Journal*, 4 (1), 5–8.

Singh, N. and Sharma, B., 2019. Role of toxicants in oxidative stress mediated DNA damage and protection by phytochemicals. *EC Pharmacology and Toxicology*, 7 (5), 325–330.

Sinha, A.K., 1972. Colorimetric assay of catalase. *Analytical Biochemistry*, 47 (2), 389–394.

Somade, O.T., *et al.*, 2018. Diallyl disulfide, an organo-sulfur compound in garlic and onion attenuates trichloromethane-induced hepatic oxidative stress, activation of NFkB, and apoptosis in rats. *Journal of Nutrition & Intermediary Metabolism*, 13, 10–19.

Toufektchan, E. and Toledo, F., 2018. The guardian of the genome revisited: p53 downregulates genes required for telomere maintenance. *Cancers*, 10 (5), 135.

Udefa, A.L., *et al.*, 2020. Antioxidant, anti-inflammatory and anti-apoptotic effects of hydro-ethanolic extract of *Cyperus esculentus* L. (tigernut) on lead acetate-induced testicular dysfunction in Wistar rats. *Biomedicine & Pharmacotherapy*, 129, 110491.

Varshney, R. and Kale, R.K., 1990. Effects of calmodulin antagonists on radiation-induced lipid peroxidation in microsomes. *International Journal of Radiation Biology*, 58 (5), 733–743.

Velki, M., *et al.*, 2019. Pesticides diazinon and diuron increase glutathione levels and affect multixenobiotic resistance activity and biomarker responses in zebrafish (*Danio rerio*) embryos and larvae. *Environmental Sciences Europe*, 31 (1), 4.

Warren, C.F., *et al.*, 2019. BCL-2 family isoforms in apoptosis and cancer. *Cell Death & Disease*, 10 (3), 177.

Wyatt, S. and Paul, W., 2008. *Organic synthesis: the disconnections approach*. 2nd ed. Oxford: Wiley Blackwell.

Yen, G.C., Lai, H.H., and Chou, H.Y., 2001. Nitric oxide scavenging and antioxidant effects of *Uraria crinita* root. *Food Chemistry*, 74 (4), 471–478.

Zhang, Y., *et al.*, 2020. The role of necroptosis and apoptosis through the oxidative stress pathway in the liver of selenium-deficient swine. *Metallomics*, 12 (4), 607–616.